REPORT DOCUMENTATION PAGE

Form Approved
OMB No. 0704-0188

1. REPORT DATE *(DD-MM-YYYY)*	2. REPORT TYPE	3. DATES COVERED *(From - To)*
Apr 06	Conference Paper	2005

4. TITLE AND SUBTITLE
Suppression of Doppler Ambiguities for Linear Sparse Arrays

5a. CONTRACT NUMBER

5b. GRANT NUMBER

5c. PROGRAM ELEMENT NUMBER

6. AUTHOR(S)
Jaime R. Roman, James C. Nelander, John W. Garnham, John D. Keisling,

*Lynn M. Black

5d. PROJECT NUMBER

5e. TASK NUMBER

5f. WORK UNIT NUMBER

7. PERFORMING ORGANIZATION NAME(S) AND ADDRESS(ES) AND ADDRESS(ES)
*Air Force Research Laboratory
Space Vehicles
3550 Aberdeen Ave SE
Kirtland AFB, NM 87117-5776

SAIC
Albuquerque, NM

8. PERFORMING ORGANIZATION REPORT NUMBER
AFRL-VS-PS-TP-2006-1015

9. SPONSORING / MONITORING AGENCY NAME(S) AND ADDRESS(ES)

10. SPONSOR/MONITOR'S ACRONYM(S)

11. SPONSOR/MONITOR'S REPORT NUMBER(S)

12. DISTRIBUTION / AVAILABILITY STATEMENT
Approved for public release; distribution is unlimited. (VS06-0025)

13. SUPPLEMENTARY NOTES
Presented at the 2006 IEEE Radar Conference, 24-27 Apr 06, Verona, NY, pp. 650-656.
Government Purpose Rights

14. ABSTRACT
A key trade-off in airborne or spaceborne synthetic aperture radar (SAR) design involves the pulse repetition frequency (PRF) and the number and location of range and Doppler ambiguities. The associated design issues are complicated further when the system involves a sparse array. A methodology is formulated based on selecting the PRF to avoid range ambiguities in the envelope mainbeam. The effects of the Doppler ambiguities falling within the envelope mainbeam are mitigated by using an optimal algorithm to generate weights that place nulls in the pattern of the (sparse or contiguous) array in the directions of the Doppler ambiguities. This approach can be used for the analysis and design of airborne or spaceborne SAR systems with contiguous or sparse arrays.

15. SUBJECT TERMS
Space Vehicles, SMART, Synthetic Aperture Radar, Pulse Repetition Frequency, Sparse Arrays, Doppler Ambiguities

16. SECURITY CLASSIFICATION OF:			17. LIMITATION OF ABSTRACT	18. NUMBER OF PAGES	19a. NAME OF RESPONSIBLE PERSON
a. REPORT	b. ABSTRACT	c. THIS PAGE			Lynn M Black
Unclassified	Unclassified	Unclassified	Unlimited	8	19b. TELEPHONE NUMBER *(include area code)* 505-846-5583

Suppression of Doppler Ambiguities for Linear Sparse Arrays

Jaime R. Roman, James C. Nelander, John W. Garnham, and John D. Keisling
SAIC
Albuquerque, NM, USA
e-mail: jaime.r.roman@saic.com

Lynn M. Black
AFRL/VSSS
Albuquerque, NM, USA
e-mail: lynn.black@kirtland.af.mil

***Abstract*— A key trade-off in airborne or spaceborne synthetic aperture radar (SAR) design involves the pulse repetition frequency (PRF) and the number and location of range and Doppler ambiguities. The associated design issues are complicated further when the system involves a sparse array. A methodology is formulated based on selecting the PRF to avoid range ambiguities in the envelope mainbeam. The effects of the Doppler ambiguities falling within the envelope mainbeam are mitigated by using an optimal algorithm to generate weights that place nulls in the pattern of the (sparse or contiguous) array in the directions of the Doppler ambiguities. This approach can be used for the analysis and design of airborne or spaceborne SAR systems with contiguous or sparse arrays.**

I. INTRODUCTION

A sparse array can arise in many contexts and can consist of many distinct configurations. One example is a large, space-based, monolithic array divided into adjacent, contiguous sub-arrays, wherein only a subset of all the sub-arrays is activated at a given time (either by design or due to element failures). Another example is a spaceborne (or airborne) constellation of platforms wherein each platform has a small, contiguous array that acts as a sub-array of the overall constellation. The methodology and algorithm presented herein for the suppression of Doppler ambiguities induced by the pulse repetition frequency (PRF) in a radar system can be extended to both of these, as well as to other cases. However, the approach is formulated and analyzed for the case of a (nominally) linear array consisting of a constellation of satellite platforms, where each satellite carries a sub-array. A set of complex-valued weights is determined optimally (based on a constrained power minimization criterion) to combine the outputs of the sub-arrays and place nulls (notches) in the directions of the known ambiguities. Timing and position errors limit the null depth and null placement capability, and both types of errors are included in simulation-based analyses of the Monte Carlo (MC) type. Single-case results are shown for a typical sparse-array pattern for the conditions of off-nominal inter-sub-array spacing with optimal weight application and without (i.e., using uniform weights). Also, MC-type results are shown for two key synthetic aperture radar (SAR) performance criteria: ambiguity ratio (AMBR) and spurious response (SPR). AMBR measures the energy detected by the sparse array in the directions of a specified number of PRF-induced Doppler ambiguities, normalized by the energy in the desired look direction. In turn, SPR is the largest single contributor to AMBR. Large AMBR reduces image contrast, whereas large SPR can produce spatially-aliased or ghost image artifacts.

The approach presented can be extended to two- or three-dimensional platform constellations. It can be extended also to accomplish joint nulling of ambiguities and interference sources, provided sufficient degrees of freedom (number of sub-arrays and weights) are available.

II. PROBLEM FORMULATION

Consider a spaceborne (or an airborne) configuration of N platforms flying as a constellation in a linear formation at constant velocity $\mathbf{v}_s$ aligned with the platforms, and with nominal uniform inter-platform spacing S (see Fig. 1). Each platform carries a radar system with an antenna array sub-system (sub-array) of width W. The sub-arrays are combined to form a large sparse array (distributed aperture). One characteristic of the array gain pattern of such a sparse array is the presence of grating lobes and nulls (or notches) at

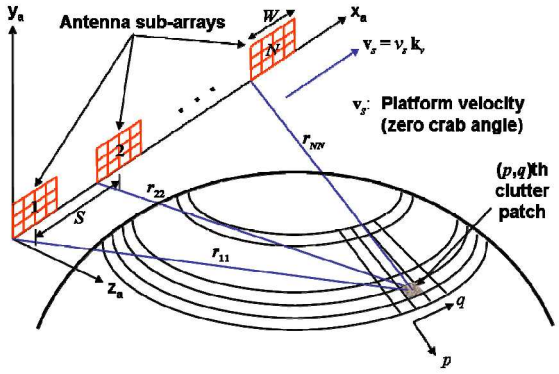

Figure 1. Scenario and platform formation for linear sparse array.

This work was carried out in support of the Space-based Multi-Aperture Research and Technology (SMART) Program at AFRL/VSSS under the direction of Ms. Lynn M. Black, Program Manager.

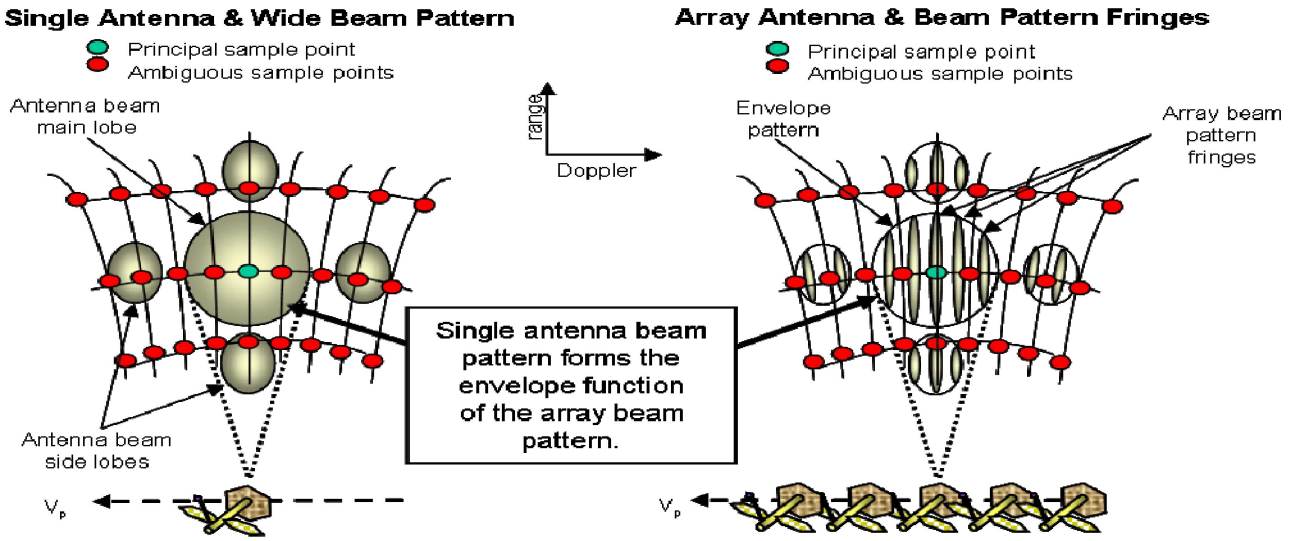

Figure 2. PRF sampling grid and antenna beam pattern.

spatial (angular) directions that are determined by the radar system and antenna parameters. In addition, for a known PRF and known platform motion, the angular directions of the ambiguities can be calculated. For such a radar system operating in the SAR mode, the system designer is faced with a trade-off between PRF and the number and location of range and Doppler-induced ambiguities [1], [2]. To address this issue, one approach is to restrict the PRF to low values so that the range ambiguities are outside the envelope mainbeam, and select the specific (low) PRF value so that the Doppler-induced ambiguities that fall inside the envelope mainbeam are in the nulls. However, in a realistic scenario, the platforms drift from their nominal relative locations, causing the array pattern to become distorted. Such distortion includes changes in the locations of the pattern grating lobes and nulls. Thus, a given Doppler ambiguity direction could fall on a grating lobe (or one of its sidelobes)

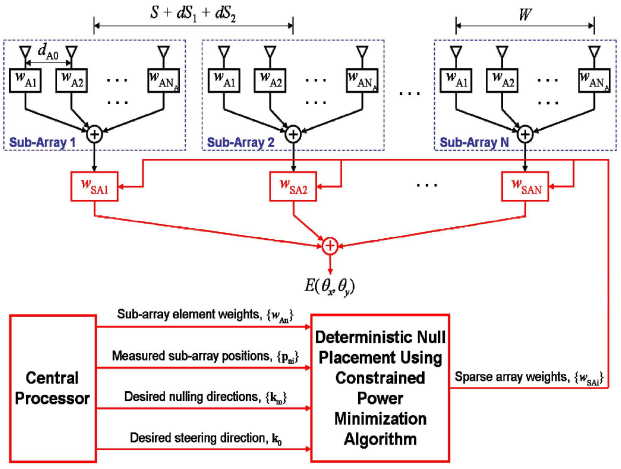

Figure 3. Linear sparse array functional block diagram.

rather than a null. The solution posed herein is to select a low PRF to avoid range ambiguities in the envelope mainbeam (as in the first part of the approach stated above), and then to mitigate the effects of the Doppler ambiguities which fall within the envelope mainbeam (see Fig. 2). This is accomplished by combining the inputs to the sub-arrays for transmission (and/or the outputs for reception) with weights $\{w_{\mathrm{SAi}}\}$ to place nulls in the pattern of the sparse array at the directions corresponding to the Doppler ambiguities (see Fig. 3). The placement of nulls to cancel signals from directions beyond the envelope mainbeam is accomplished via the appropriate selection of the sub-array weights, $\{w_{\mathrm{An}}\}$ (this case is not considered here).

Fig. 4 defines the antenna array coordinate frame for the sparse array and key antenna parameters, with r_{ii} being the range from the ith sub-array to the center of the region of interest (ROI) (see also Fig. 1). It can be shown that the Doppler ambiguities occur at the set of angles (for $\theta_{0y} = 90°$)

$$\theta_{mx} = \cos^{-1}\left[\cos(\theta_{0x}) + \frac{m\lambda_0 f_{\mathrm{PR}}}{2v_{\mathrm{s}}}\right] = \cos^{-1}\left[\left(f_{\mathrm{DC}} + m f_{\mathrm{PR}}\right)\left(\frac{\lambda_0}{2v_{\mathrm{s}}}\right)\right]$$
$$m = m_{\min}, \ldots, m_{\max} \quad \text{and} \quad m \neq 0\,. \qquad (1)$$

Also, λ_0 is the nominal (center) wavelength, f_{PR} is the PRF, v_{s} is the platform speed, θ_{0x} is the $\mathbf{x}_{\mathrm{a}}$-axis cone pointing angle, $f_{\mathrm{DC}} = 2v_{\mathrm{s}}\cos(\theta_{0x})/\lambda_0$ is the Doppler frequency of the scene center clutter patch towards which the array is pointed, and $m_{\min}$ and $m_{\max}$ are integers specified to include all the Doppler ambiguity directions enclosed by the array envelope mainbeam. For boresight-looking conditions, $\cos(\theta_{0x}) = \cos(90°) = 1$, $f_{\mathrm{DC}} = 0$, and $-m_{\min} = m_{\max} = M_{\mathrm{E}}/2$ since the ambiguity directions are symmetric about the boresight. Here M_{E} denotes the total number of ambiguities inside the

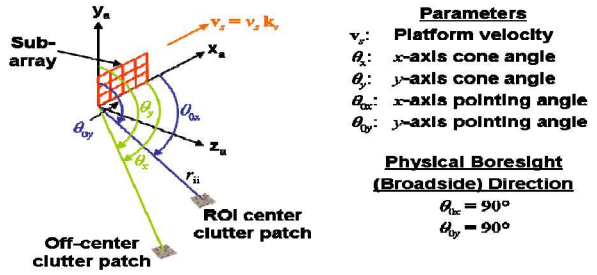

Figure 4. Antenna sub-array coordinates and parameter definitions.

array envelope mainbeam. In general, only a subset of all the M_E intra-mainbeam ambiguities is to be nulled. This is true, for example, when those ambiguities close to the first envelope null are attenuated sufficiently already. To account for that condition, let $M \le M_E$ denote the number of intra-mainbeam ambiguities to be nulled.

The objective is to place a null in the array gain pattern $G(\theta_x,\theta_y)$ at each of the M specified PRF-induced Doppler ambiguity directions using a set of linear weights (in place of the nominal uniform weights), while maintaining the general integrity of the rest of the pattern and specifically maintaining the beam gain in the required look direction. This objective is achieved by minimizing the power received from the specified directions and imposing an appropriate set of linear equality constraints on the weight vector. These requirements lead to a constrained minimization problem which admits a closed-form analytic solution for the conditions specified. Let $\boldsymbol{\varepsilon}$ denote an M-element column vector representing the signal received from the M specified ambiguity directions,

$$\boldsymbol{\varepsilon} = \mathbf{H}\mathbf{w}_{SA} \tag{2}$$

where $\mathbf{w}_{SA}$ is the unknown N-element complex-valued column vector of sparse array weights, and $\mathbf{H}$ is an MxN complex-valued matrix representing the array model. Matrix $\mathbf{H}$ includes the sub-array antenna characteristics (determined by the sub-array weights $\{w_{An}\}$ shown in Fig. 3) and includes phase and position errors for the sparse array.

Minimization of the received power in the M ambiguity directions is represented by a performance index $J(\mathbf{w}_{SA})$ of the form

$$J(\mathbf{w}_{SA}) = \|\boldsymbol{\varepsilon}\|^2 = \|\mathbf{H}\mathbf{w}_{SA}\|^2 = \mathbf{w}_{SA}^H \mathbf{H}^H \mathbf{H}\mathbf{w}_{SA}\,. \tag{3}$$

Also, let $L_1(\mathbf{w}_{SA})$ denote a linear equality constraint to force unity gain in the desired look direction, denoted as $\mathbf{h}_0$ (assuming $G(\theta_{0x},\theta_{0y})$ is normalized to unity):

$$L_1(\mathbf{w}_{SA}) = \mathbf{w}_{SA}^H \mathbf{h}_0 - 1 = \mathbf{h}_0^H \mathbf{w}_{SA} - 1 = 0\,. \tag{4}$$

Furthermore, let $L_2(\mathbf{w}_{SA})$ denote a power equality constraint on the weight vector of the form

$$L_2(\mathbf{w}_{SA}) = \mathbf{w}_{SA}^H \mathbf{w}_{SA} - \rho_o = 0 \tag{5}$$

where ρ_o is an unspecified real-valued scalar that represents the radius of a hypersphere in N-dimensional space. This constraint leads to a solution that involves diagonal loading (or regularization), which allows inversion of an ill-conditioned matrix, a case that can arise in this type of problem.

III. Problem Solution

The constrained optimization problem defined above is re-formulated by defining a Hamiltonian function as [3]

$$H(\mathbf{w}_{SA},\mu_1,\mu_2) = J(\mathbf{w}_{SA}) + \mu_1 L_1(\mathbf{w}_{SA}) + \mu_2 L_2(\mathbf{w}_{SA}) \tag{6a}$$

$$\begin{aligned} H(\mathbf{w}_{SA},\mu_1,\mu_2) = {} & \mathbf{w}_{SA}^H \mathbf{H}^H \mathbf{H}\mathbf{w}_{SA} + \mu_1\left(\mathbf{w}_{SA}^H \mathbf{h}_0 - 1\right) \\ & + \mu_2\left(\mathbf{w}_{SA}^H \mathbf{w}_{SA} - \rho_o\right) \end{aligned} \tag{6b}$$

where μ_1 and μ_2 are Lagrange multipliers (unknown real-valued scalars). In a well-posed problem, all terms are real-valued scalar functions of the complex-valued vector $\mathbf{w}_{SA}$. The values for $\mathbf{w}_{SA}$, μ_1, and μ_2 that minimize the unconstrained Hamiltonian also minimize the performance index (3) subject to the equality constraints (4) and (5). The analytic solution to this formulation is obtained as [4]

$$\mathbf{w}_{SA} = \frac{1}{\mathbf{h}_0^H\left(\mathbf{H}^H\mathbf{H} + \mu\,\mathbf{I}_N\right)^{-1}\mathbf{h}_0}\left(\mathbf{H}^H\mathbf{H} + \mu\,\mathbf{I}_N\right)^{-1}\mathbf{h}_0\,. \tag{7}$$

In (7) the multiplier μ_2 has been replaced by μ (without the subscript) in order to simplify notation. Here μ remains as a parameter that is varied numerically in order to optimize the solution with respect to various considerations. Parameter μ is referred to in the literature as the diagonal loading coefficient, and its most common use is to provide numerical stability to the matrix inversion in (7) when the matrix product $\mathbf{H}^H\mathbf{H}$ is rank-deficient. Such a condition occurs in the context herein when $M < N$. Equation (7) is obtained alternatively using a performance index that has an additive second term of the form $\mu\,\|\mathbf{w}_{SA}\|^2$ and a single linear equality constraint $L_1(\mathbf{w}_{SA})$. This corresponds to treating the power term as a "soft" constraint.

The approach presented can be extended to implement joint cancellation of ambiguities and interference sources within the envelope mainbeam by including the interference source directions in the formulation (2) via an enhanced

vector $\boldsymbol{\varepsilon}$. In most realistic scenario conditions, the directions of the interference sources are unknown and have to be estimated. This introduces into the weight expression a (spatial) covariance matrix for those sources, and such a matrix has to be estimated in an adaptive manner.

IV. Simulation-Based Results

A MATLAB-based simulation was generated to assess the performance of the algorithm in the presence of errors in the measurement of phase and position. Sparse array gain patterns for several cases have been analyzed. These include: (a) nominal case (linear uniform array with uniform weights); (b) distorted-pattern case (linear non-uniform array with uniform weights); and (c) null-steered case (linear non-uniform array with optimal weights calculated to place nulls at the specified M ambiguity directions). The weights are calculated for a linear array that includes non-uniform inter-element spacing as well as measurement errors (as calculated by an on-board processor), and they are applied to the same linear non-uniform array but without the errors (also representing on-board operation). AMBR and SPR as functions of position and/or phase errors have been determined. The results shown are for a feasible set of system parameters in a space-based low Earth orbit (LEO) scenario, with key parameters listed in Table 1 and in the figures.

Figs. 5 through 7 present a 1.5-degree extent of the nominal, distorted, and null-steered (for M = 4) one-way array radiation patterns, respectively. The distorted pattern (Fig. 6) and the null-steered pattern (Fig. 7) were generated for a randomly-chosen realization of phase error with standard deviation (sd) of 9.0 deg, position offset error along the $\mathbf{x}_a$-axis direction with sd of 0.00075 m, and position offset along the $\mathbf{x}_a$-axis direction with sd of 2.0 m. In all three figures the angular directions of the PRF-induced Doppler ambiguities are shown as green vertical lines. Notice that the distorted pattern is similar to the nominal pattern only for a few grating lobes close to the center. The deviation from nominal at a given pattern direction increases as the non-uniformity increases (larger position offset sd). This behavior is typical for a distorted pattern. Notice also that the selected PRF induces the third ambiguity (from the center) to fall on the envelope pattern null (dashed red curve), so only $M = 4$ nulls have to be placed for this design.

TABLE I. Key Simulation Parameters and Their Values.

Parameter	Value
Platform speed, v_s	7,158.468 m/s
Orbit altitude, h_s	1,000.0 Km
Squint angle	60.0 deg
Grazing angle	24.0 deg
Sub-array width, W	4.0 m
Sub-array height, H	4.0 m
Nominal inter-sub-array separation, S	40.0 m
Lateral position offset bound, ΔS	5.0 m
Sub-array weighting, $\{w_{An}\}$	uniform
No. of sub-array weights, N_A	268
Pulse repetition frequency (PRF), f_{PR}	1,188.0 Hz
Radiation wavelength, λ_0	0.03 m
No. of sparse array weights, N	10
No. of ambiguities to be nulled, M	4
No. of ambiguities within envelope mainbeam, M_E	6
No. of ambiguities for AMBR calculations, M_A	6
$\mathbf{x}_a$-axis pointing cone angle, θ_{0x}	66.7425 deg
$\mathbf{y}_a$-axis pointing cone angle, θ_{0y}	127.84 deg
No. of independent MC realizations	10,000
Position offset standard deviation, σ_S	2.0 m
Position offset error standard deviation, σ_x	variable
Phase error standard deviation, σ_ϕ	variable

In Fig. 7, notice that the null-steered pattern is asymmetric with respect to the pointing direction (center). This is the result of applying weights designed for an array with included measurement errors to an array without errors, which represents the condition of realistic on-board operation. Another effect due to the presence of errors is that the depth of the desired nulls is typically between 5 and 25 dB deeper than without nulling. In contrast, for a system without errors the nulls are much deeper.

AMBR and SPR can be measured over a set of ambiguities larger or smaller than the set of ambiguities inside the envelope pattern (M_E), and also larger or smaller than the set of ambiguities to be nulled (M). To account for that, let M_A denote the number of ambiguities used for the calculation of AMBR and SPR. For the specific cases shown in Figs. 6 and 7, the null-steered pattern one-way AMBR for the six ambiguities bounding the mainbeam (M_A = 6) is –23.17 dB, a considerable improvement over the AMBR of the pattern without nulling, which is –12.18 dB. For the same ambiguities, the null-steered pattern one-way SPR is –51.72 dB, in contrast to –32.94 dB without nulling.

Fig. 8 shows a two-dimensional contour plot (top) of the null-steered two-way beam pattern projected onto the ground at scene center (the (0,0) point), along with a one-dimensional slice (bottom) along the range line of scene center. The Doppler ambiguity positions are shown by the red lines on the lower plot; the corresponding nulls appear as dark blue lines (at a slant angle due to off-boresight pointing) in the contour plot. Fig. 9 is a closer view of the contour plot near the first Doppler ambiguity, which allows visualization of the lobe-like structure detail in the null ditch.

Figs. 10 and 11 present AMBR and SPR, respectively, vs. phase and position offset errors for a MC analysis using 10,000 statistically-independent trials. In these results M_A = 6 also. The median and the 95th percentile curves are shown for the distorted (black curves) and null-steered (red curves) cases. In both figures, the abscissa represents a dimensionless parameter; thus phase and position errors vary jointly. These types of plots can be used to establish system performance requirements. A typical constraint for AMBR or SPR is shown in each respective figure. The curves in Fig. 10 suggest, for example, that to achieve AMBR $\leq$ –20 dB for 95% of the cases, phase error is restricted to have a sd

of ~12.0 deg (which translates into a position error of $\lambda/30$), and position offset error is jointly restricted to having a sd of approximately $\lambda/30$. Analogously, from Fig. 11 it can be deduced that in order to achieve an SPR ≤ -30 dB for 95% of the cases, the phase error must be restricted to a sd of ~9.4 deg (which translates into a position error of $\lambda/38$), and position offset error must be jointly restricted to a sd of approximately $\lambda/38$.

V. Summary and Conclusions

An approach is presented for handling PRF-induced ambiguities in sparse array radar systems. Specifically, a low PRF value is selected to avoid range ambiguities in the envelope mainbeam, and the effects of the Doppler ambiguities which fall within the envelope mainbeam are mitigated by combining the inputs to the sub-arrays with weights to place nulls in the pattern of the sparse array at the directions corresponding to those Doppler ambiguities. An optimal (constrained power minimization) criterion is formulated and solved for the generation of the weights. Selected performance results demonstrate the applicability of the criterion for system analysis and design of SAR systems. The formulation and all results are presented in the context of uniform linear sparse arrays but can be extended to two- or three-dimensional sparse arrays.

The approach presented can be used effectively for the analysis and design of airborne or spaceborne SAR systems that consist of contiguous or sparse array configurations. In addition, it can be extended to the joint nulling of ambiguities and interference sources.

References

[1] R. W. Bayma and P. A. McInnes, "Aperture size and ambiguity constraints for a synthetic aperture radar," IEEE 1975 Int'l. Radar Conf. Record, 21-23 April 1975, pp. 499–504.

[2] F. K. Li and W. T. K. Johnson, "Ambiguities in spaceborne synthetic aperture radar systems," IEEE Trans. Aero. and Electr. Systems, vol. AES-19, no. 3 (May 1983), pp.389–396.

[3] M. Athans and P. L. Falb, Optimal Control, McGraw-Hill Book Co., New York, NY, 1966.

[4] J. E. Hudson, Adaptive Array Principles, IEE, UK, jointly with Peter Peregrinus Ltd., Stevenage, UK, 1981.

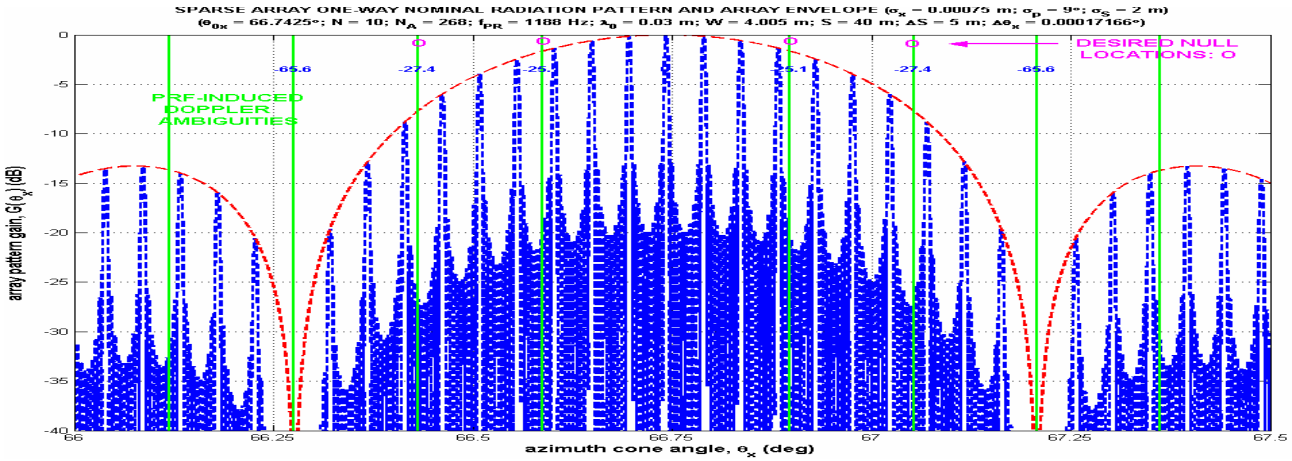

Figure 5. Nominal array gain pattern (1.5-degree extent).

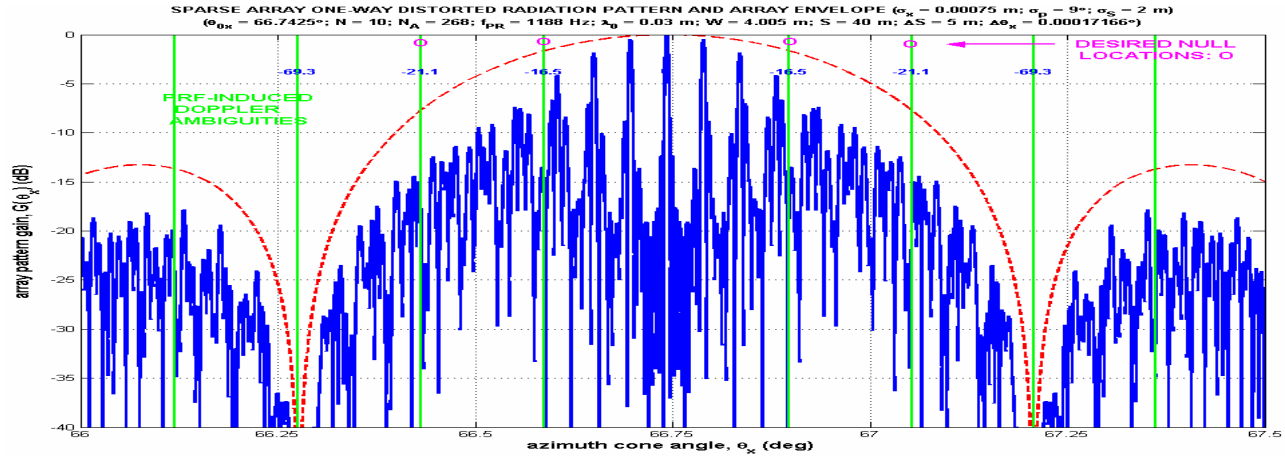

Figure 6. Distorted array gain pattern (1.5-degree extent).

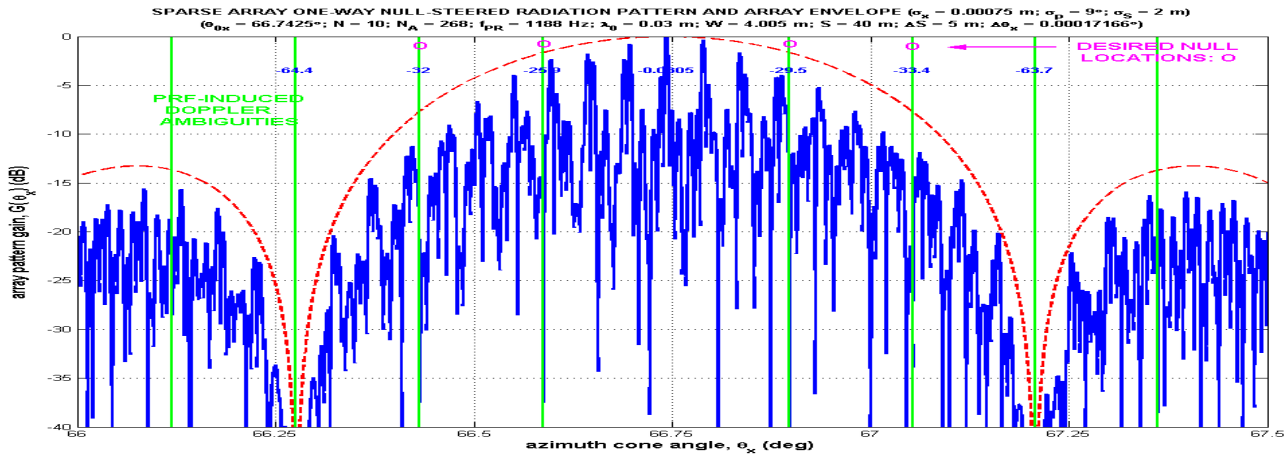

Figure 7. Null-steered array gain pattern (1.5-degree extent).

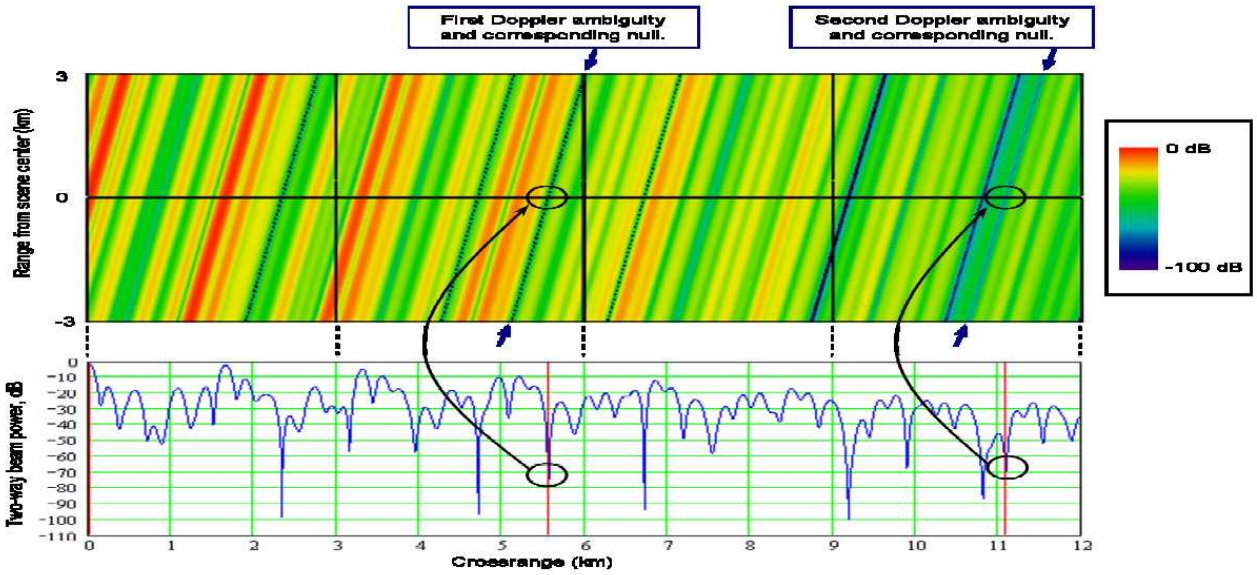

Figure 8. Two-way null-steered beam pattern showing Doppler ambiguity locations. The upper plot is a contour plot looking down on the radar scene. The lower plot is a slice along the range line of scene center (at 0 km).

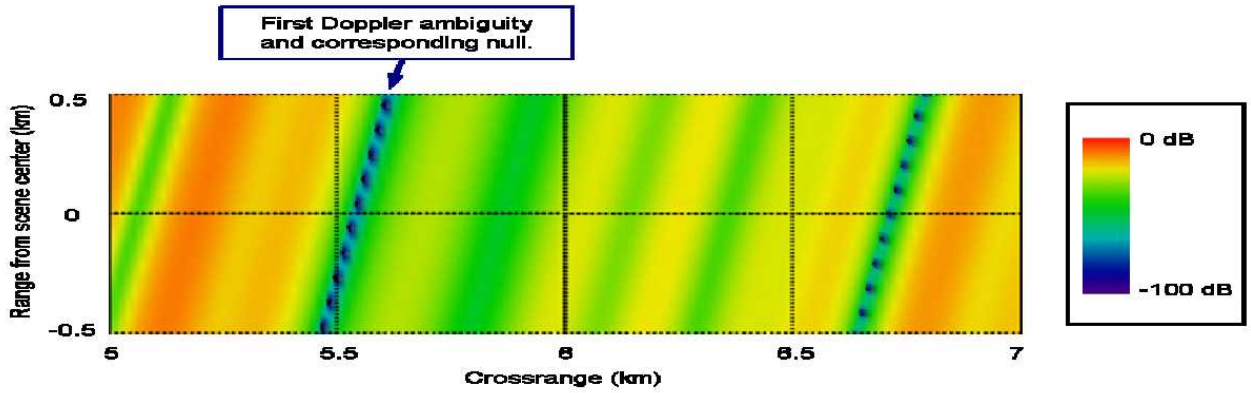

Figure 9. Magnified contour plot of Figure 8.

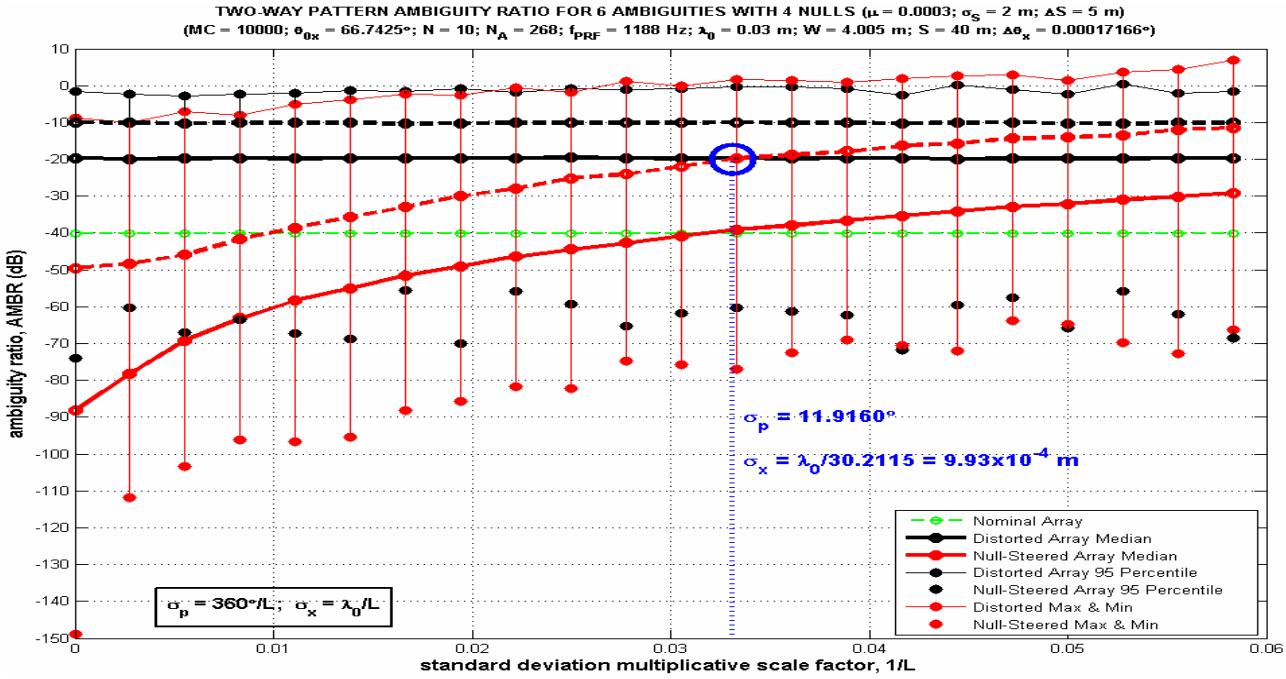

Figure 10. AMBR vs. phase and position offset errors: Monte Carlo analysis results.

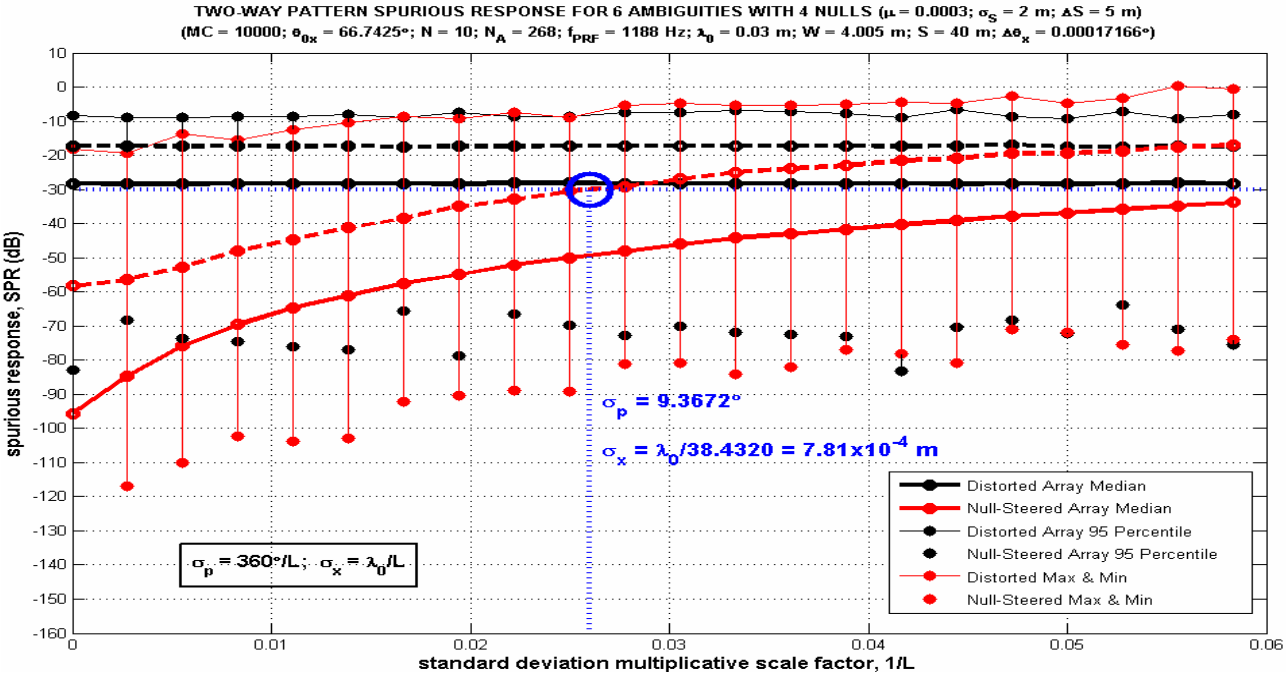

Figure 11. SPR vs. phase and position offset errors: Monte Carlo analysis results.